

Effect of entry bending moment on exit curvature in asymmetrical rolling

Fatemeh Farhatnia¹, M. Salimi^{2*}

¹ Engineering Faculty, Islamic Azad University, Khomeini-shahr Branch, Isfahan, IRAN

^{2*} Department of Mechanical Engineering, Isfahan University of Technology, Isfahan, 8415683111 IRAN

*Corresponding Author: e-mail: salimi@cc.iut.ac.ir, Tel +98-311-3915214, Fax+98-311-3912625

Abstract

This paper investigates the asymmetrical rolling process using the Modified Slab Method. Elastic-plastic and linear work hardening material was assumed. In solving the equilibrium equations, the difference in roll pressure distribution was assumed linear. Using this model rolling parameters such rolling force, torque and the developed curvature were easily calculated. Simulation results indicated that for decreasing warping in an asymmetrical rolling, bending moment can be applied in suitable direction. In addition, employing a bending moment at entry of the roll gap in a symmetrical rolling process causes pressure difference on the rolls and warping at the outlet, as happens in an asymmetrical rolling process. Similarly, increasing the roll diameter ratio increases the pressure differences, but the average pressure between the sheet and the rolls is decreased while by increasing the reduction in thickness the average pressure is increased.

Keywords: Asymmetrical Rolling; Modified Slab Method; Pressure Difference; Rolling Force; Bending Moment.

1. Introduction

In practice, rolling of plate and sheet asymmetry arises due to inequality in roll radii, roll velocity and interface friction. These variations may cause the outgoing plate to bend in upward or downward directions. Actually, one of many difficulties appearing during asymmetrical rolling process is band bending at exit from a deformation zone. An effect of non-uniform deformation is bending up or down at the outlet. This can cause damage to the table rollers and difficulty in next roll pass entry. Significant curvature of the band can cause breaking of the rolling process. Recently this type of rolling has become more important because it requires less rolling force and torque. A few researchers have carried out experimental investigations and theoretical analyses to study the effect of asymmetrical rolling. Some papers are not essentially able to predict the developed curvature. Only a few researchers were able to predict the developed curvature through complex and time-consuming computations.

Chekmarev et al. (1956) carried out the experimental research on rolling of aluminum, lead and steel sheets. Their observations indicated that employing asymmetrical rolling reduced the rolling force as much as 40%. Collins et al. (1975) presented a solution based on slip line field method and compared the results with experimental data. Pan et al. (1982) used upper bound method in order to calculate the sheet warping. Their results showed that by employing the front tensile force the product curvature would be reduced. Kiuchi et al. (1986) used the same technique to analyze the process. They predicted the sheet warping as well as the other asymmetrical rolling characteristics. Dyja et al (1994) found that in an asymmetrical rolling for speed ratio of about 1.05, the average pressure applied on the workpiece is reduced by 15%. Hwang et al. (1996) attempted to analyze the asymmetrical rolling by using the stream function method. They investigated the influence of thickness reduction in presence of roller speed mismatch on outgoing curvature. According to their analysis, when the speed ratio is smaller than one, the curvature will be positive. It means that the plate bends toward the roller with higher speed. In addition, they concluded the radius of curvature is sensitive to variations of radius ratios. In the other research, Hwang et al. (1997) developed an analytical model based on the slab method assuming constant shear friction between the rolls and the sheet. Their model did not account for the developed curvature. Richelsen (1997), Shivpuri et al. (1988) and Lu et al. (2000) used finite element method to estimate the rolling force, the rolling torque and the developed curvature. Richelsen investigated the effect of initial thickness and roughness ratio of rollers on sheet bending. For this purpose, she studied two-dimensional viscoelastic-plastic behavior of the sheet in a finite element simulation. Wanheim and Bay's friction model was incorporated in her FE model. She concluded that by increasing the thickness reduction

the neutral points displaces toward the exit and increases the frictional stress between the sheet and rollers. Salimi et al. (2002) used modified slab method to analyze the asymmetrical plate rolling and to predict strip curvature. Knight et al. (2003 & 2005) considered a rigid-plastic model of continuous hot rolling of low carbon steel under unequal friction coefficients using ABAQUS commercial software. According to their observations, in the first pass low carbon steel sheet tends to warp toward roller with slower speed and in the next passes it bends toward faster speed one. They concluded that applying lubricant to the plate reduces the warping effectively. That was a proof for influence of rollers friction coefficient on sheet curvature. Farhatnia et al. (2005 & 2006) studied the effect of different factors on rolling force, torque and warping in the clad sheet rolling process that is one of the classifications in asymmetrical rolling, by applying Modified Slab Method. In addition, Farhatnia et al. (2006) carried out a numerical simulation on asymmetrical rolling based on ALE technique in Finite Element Method. Mousavi et al. (2007) performed finite element simulation using ABAQUS commercial software package. Their results indicated that by increasing the length of the shear zone the sheet curvature did not necessarily increase. The sheet curvature also depends on the plastic strain distributions and the shape factor. Gudur et al. (2007) presented a method for estimating the friction coefficient based on the asymmetric rolling operation. They developed a slab method based computer code for estimating the curvature of the rolled sheet under asymmetric conditions by incorporating Wanheim and Bay's friction model. The internal moment was ignored and free entry without any restraint was assumed. They concluded that when the asymmetry due to speed mismatch is considered, the strip curls towards the slower rotating roll; however, the magnitude of the curvature depended on the friction coefficient of rollers. They solved the inverse problem of finding out the coefficient of friction for a given the radius of curvature using the bisection method.

In present work, a mathematical model is developed which allows the complete inclusion of asymmetric deformation effects through three equation of equilibrium. The effect of shear stress across the thickness is considered. By simultaneously solving three equilibrium equations, characteristics of asymmetrical rolling are derived. The modified slab method is employed to consider the effects of variations in roll radii, reduction, forward and backward tensions, work rolls speed mismatch, interface friction and bending moment at entry. For this purpose, the equation of internal bending moment distribution is derived. For the first time, the influence of bending moment on outgoing curvature is considered in this paper. It is also shown that how the application of bending moment at entry changes the characteristics of rolling from symmetrical to asymmetrical condition.

2. Modeling and equilibrium equations

Figure 1 shows the schematic diagram of asymmetrical rolling. The deformation zone is divided into 3 distinct zones. In zone I and III both frictional stresses on the upper and lower rolls are either forward or backward. In zone II (the cross shear region), the frictional stresses on upper and lower side are in opposite directions. Following are the basic assumption in building up the model.

1. The work rolls are rigid.
2. Elastic-plastic and linear work hardening material is assumed.
3. The plastic deformation is plane strain.
4. Frictional stresses at interfaces are functions of the material yield stress and friction coefficient.
5. The contact length is small compare to the circumference of the rolls.

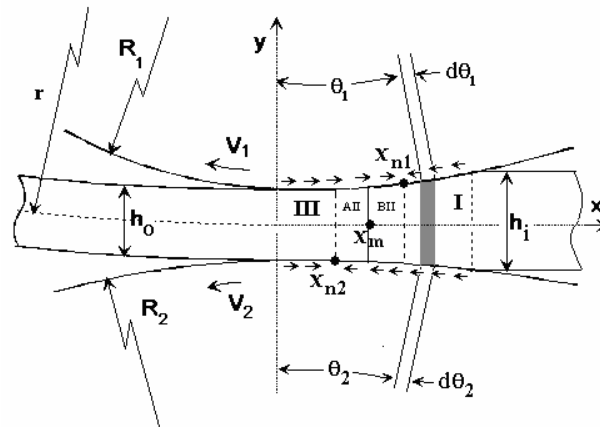


Figure 1. Schematic illustration of asymmetrical rolling

Referring to Figure 2, the mathematical expressions of equilibrium for the slab element are given by the three following equations:

$$\begin{aligned}
 d(hq) + [-(\tau_1 + \tau_2) + p_1 \tan \theta_1 + p_2 \tan \theta_2] dx &= 0 \\
 d(h\tau) + [(-\tau_1 \tan \theta_1 + \tau_2 \tan \theta_2) - (p_1 - p_2)] dx &= 0 \\
 dM + \frac{h}{2} [(p_1 \tan \theta_1 - p_2 \tan \theta_2) + (\tau_1 - \tau_2) - 2\tau] dx &= 0
 \end{aligned}
 \tag{1}$$

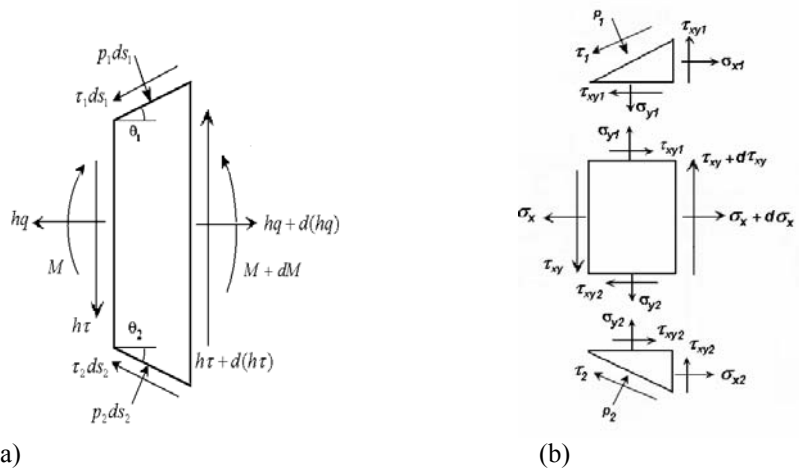


Figure 2. (a) External load acting on the vertical element in zone I

(b) Assumed stress system for infinitesimal triangular elements

Defining the mean pressure “p” and the pressure difference “Δ” by the following relations:

$$p_1 + p_2 = 2p, \quad p_1 - p_2 = \Delta \tag{2}$$

The three equilibrium equations take the form:

$$dq = -\frac{1}{h} \left[\frac{1}{2} \left(\frac{1}{R_1} - \frac{1}{R_2} \right) \Delta + (p + q) \left(\frac{1}{R_1} + \frac{1}{R_2} \right) \right] x - (\tau_1 + \tau_2) dx$$

$$d(h\tau) = \Delta dx - \left(-\frac{\tau_1}{R_1} + \frac{\tau_2}{R_2} \right) x dx \tag{3}$$

$$dM + (\tau_1 - \tau_2) \frac{h}{2} dx = h\tau dx - \frac{h}{2} \left\{ \frac{1}{2} \left(\frac{1}{R_1} + \frac{1}{R_2} \right) \Delta + p \left(\frac{1}{R_1} - \frac{1}{R_2} \right) \right\} x dx$$

The above equilibrium differential equations may be rearranged as follows:

$$\begin{cases} d(qh) + \left\{ \tau_e + \left(I_4 \Delta + \frac{2}{R_m} (p + q) \right) x \right\} dx = 0 \\ d(h\tau) + (\tau'_e x - \Delta) dx = 0 \\ dM_b + \left\{ h\tau + \frac{h}{2R_m} \Delta x + \tau'_e \frac{h}{2} \right\} dx = 0 \end{cases} \tag{4}$$

where R_m is the average diameter $R_m = \left(\frac{2R_1R_2}{R_1 + R_2} \right)$ and $I_4 = \frac{1}{2} \left(\frac{1}{R_1} - \frac{1}{R_2} \right)$.

In zone I: $\tau_e = + (\tau_1 + \tau_2)$, in zone II $\tau_e = + (\tau_1 - \tau_2)$ and in zone III: $\tau_e = - (\tau_1 + \tau_2)$. For small reduction per pass $\tan \theta_1 \approx \frac{x}{R_1}$, $\tan \theta_2 \approx \frac{x}{R_2}$ and $l = \sqrt{R_m(h_i - h_o)}$.

2.1. Yield criterion

Using the same approach as described by Salimi et al. (2002) the yield criterion for a vertical slab element is given as follows:

$$\bar{\sigma}_x - \bar{\sigma}_y = \sigma_f \left(\sqrt{\frac{1 - m_1^2 c_1^2}{3}} + \sqrt{\frac{1 - m_2^2 c_2^2}{3}} \right) \tag{5}$$

Where $\bar{\sigma}_x$ and $\bar{\sigma}_y$ are the average normal stresses in x and y directions. Friction coefficients between the upper roll and that of lower rolls (m_1 and m_2) may be different but it is assumed to remain constant along the contact length of the work-piece and the rolls. They introduced constants c_1, c_2 and showed that these values depend on parameters such as the roll gap geometry and are

the average shear stress through thickness to that of the surface shear stresses. The horizontal and vertical equilibrium equations for the differential triangular elements are given by:

$$(\sigma_{x1} + p_1) \tan \theta_1 - (\tau_1 + \tau_{xy1}) = 0 \tag{6-1}$$

$$(\tau_{xy1} - \tau_1) \tan \theta_1 - (\sigma_{y1} + p_1) = 0 \tag{6-2}$$

Writing similar equations for the lower portion and combining the equations we have:

$$\bar{\sigma}_x - \bar{\sigma}_y = p + q - \left(\frac{\tau_1}{R_1} - \frac{\tau_2}{R_2} \right) x \tag{7}$$

Depending on the zone considered, values in the parenthesis change sign. The general form of the above equation is given by the following equation:

$$p + q = I_1 + I_2 x \tag{8}$$

By referring to equations 9 and 11, I_1 and I_2 are given by:

$$I_1 = \sigma_f \left(\sqrt{\frac{1 - m_1^2 c_1^2}{3}} + \sqrt{\frac{1 - m_2^2 c_2^2}{3}} \right) \tag{9}$$

Constant c_1 and c_2 depend on parameters such as the roll gap geometry and are the average shear stress through thickness to surface shear stresses as defined by Salimi et al. (2002).

$$I_2 = \begin{cases} -\frac{\tau_1}{R_1} + \frac{\tau_2}{R_2} & \text{zone I} \\ \frac{\tau_1}{R_1} + \frac{\tau_2}{R_2} & \text{zone II} \\ \frac{\tau_1}{R_1} - \frac{\tau_2}{R_2} & \text{zone III} \end{cases} \tag{10}$$

3. Method of solving the differential equation

The unknowns of the differential equilibrium equation are M , Δ , τ , q and p . Previous theoretical and experimental investigations have shown that the distribution of the roll pressure difference with respect to the distance from the neutral point is linear. In this paper this distribution for the entry and exit regions are assumed as follows:

$$\frac{\Delta}{k} = -\frac{a_1 h_m}{l^2} (x_m - x) \quad 0 \leq x \leq x_m \tag{11}$$

$$\frac{\Delta}{k} = -\frac{a_2 h_m}{l^2} (x_m - x) \quad x_m \leq x \leq x_o \tag{12}$$

In these relations \bar{k} and x_m are the mean yield stress and the point at which the pressure difference vanishes, respectively. As an approximation, the location of this point is considered to be at the center of the cross shear region, i.e. $x_m = (x_{n1} + x_{n2})/2$. While h as sheet thickness depends to the distance from the exit, $h = h_o + x^2/R_m$ and h_m is the average thickness. Substituting the above relations into the equilibrium equations, the shear force (τh), the mean tension to the strip (q) and the bending moment (M_b) for the entry region are expressed as:

$$\tau h = \frac{-ah_m k}{2l^2} (x - x_m)^2 - \tau'_e \frac{x^2}{2} + c_\tau \tag{13-1}$$

$$q = J_{1q} + J_{2q} \ln(h_m R_m + x^2) + J_{3q} \tan^{-1} \left(\frac{x}{\sqrt{R_m h_m}} \right) + c_q \tag{13-2}$$

$$\begin{aligned}
 M_b = & \frac{ah_m k}{6l^2} (x - x_n)^3 + \frac{\tau' x^3}{6} - c_\tau x - \frac{\tau_e''}{2} \left(h_m x + \frac{x^3}{3R_m} \right) + \frac{ah_m k}{2R_m l^2} \left\{ \frac{h_m x^3}{3} - \frac{h_m x_m x^2}{2} + \frac{x^5}{5R_m} - x_m \frac{x^4}{4R_m} \right\} \\
 & + (c_q - I_1) \left(\frac{h_m x^2}{2} + \frac{x^4}{4R_m} \right) + (J_{1q} - I_2) I_4 \left(h_m \frac{x^3}{3} + \frac{x^5}{5R_m} \right) + J_{2q} I_4 \left\{ \frac{h_m R_m}{4} \left(h_m + \frac{2x^2}{R_m} \right) (\ln(h_m R_m + x^3)) \right. \\
 & \left. \frac{x^5}{5R_m} \right\} + J_{2q} I_4 \left\{ \frac{h_m R_m}{4} \left(h_m + \frac{2x^2}{R_m} \right) (\ln(h_m R_m + x^3)) - 1 + \frac{x^4}{4R_m} \ln(h_m R_m + x^2) + \frac{x^4}{8R_m} \right\} + J_{3q} I_4 \\
 & \left\{ \tan^{-1} \left(\frac{x}{\sqrt{R_m h_m}} \right) \left(\frac{x^2}{R_m} + 2h_m \right) x^2 - \frac{1}{12} x^3 \sqrt{\frac{h_m}{R_m}} - \frac{1}{4} x \sqrt{R_m h_m} + \frac{1}{4} h_m^2 R_m \tan^{-1} \left(\frac{x}{\sqrt{R_m h_m}} \right) \right\} + c_M
 \end{aligned} \tag{13-3}$$

Coefficients J_{1q} , J_{2q} , J_{3q} , in the second equation are defined as follows:

$$\begin{aligned}
 J_{1q} &= -2I_2 + \frac{ah_m k I_4 R_m}{l^2} \\
 J_{2q} &= \frac{-I_4 ah_m R_m x_m}{2l^2} - I_1 \\
 J_{3q} &= \sqrt{\frac{R_m}{h_m}} \left(-\tau_e + 2h_m I_2 + \frac{ah_m^2 k I_4 R_m}{l^2} \right) \\
 I_4 &= \frac{1}{2} \left(\frac{1}{R_1} - \frac{1}{R_2} \right)
 \end{aligned} \tag{14}$$

τ_e , τ_e' and τ_e'' are parameters related to the friction appeared at different regions accordingly. c_τ , c_q and c_M are constants, which are determined by applying the boundary conditions for the shear stress, front/back tension and bending moments to the element in different regions. x_{n1} , x_{n2} , a_1 and a_2 are the unknown values, if these unknowns are calculated the neutral point location and the stress distributions can be determined easily. To determine these values, four distinct equations are required. These equations are derived from the continuity conditions of the shear stress, the strip tension, the internal moment at two adjacent regions and the volume constancy. In pressure difference equations at the entry ($0 \leq x \leq x_m$) and exit ($x_m \leq x \leq x_o$) regions (equation 11 and 12), the coefficients a_1 and a_2 are different, the cross shear region are divided into two distinct zones A and B.

By imposing the continuity equations at $x = x_m$; $(\tau h)^A = (\tau h)^B$, $q^A = q^B$ and $M_b^A = M_b^B$ together with the volume constancy equation; $x_1 = R_m \sqrt{\frac{v_2 x_2^2}{v_1 R_m} + \left(\frac{v_2}{v_1} - 1\right) \frac{h_o}{R_m}}$ four equations are derived. By solving them, the unknowns x_{n1} , x_{n2} , a_1 and a_2 are obtained.

4. Determination of output curvature

As the material behaviour is considered as elastic-plastic and linear work hardening one, the shear strain at any point is the summation of the elastic and plastic strain given by:

$$d\gamma_{xy} = d\gamma_{xy}^e + d\gamma_{xy}^p = \frac{d\tau_{xy}}{G} + \tau_{xy} \frac{d\varepsilon_y}{\sigma_y'} \tag{15}$$

where σ_y' is the stress deviation.

Method of calculating the developed curvature due to the shear strain is the same as the method given by Salimi et al. (2002) In addition to the effect of the shear strain on the sheet, the effect of the bending moment along the arc of contact has to be considered.

4.1 Curvature due to internal bending moment

To evaluate the curvature imposed on the sheet due to the bending moment in any deformation zone, it is assumed that a crossing sheet through the roll gap may be considered as a beam with variable thickness subjected to external loading. The distribution of

internal reactions (bending moments, shear and axial forces) has to be obtained. Due to variation in sheet thickness and for simplicity in calculations the mean thickness of the plate at any region is employed as the beam height (\bar{h}_i), the average thickness is changed stepwise in the entire deformation zone. Generally, the mean thickness in domain $a < x < b$, is obtained as follows:

$$\bar{h} = \frac{\int_a^b h dx}{b-a} \tag{16}$$

Hence, for the entire deformation zone, the average thickness \bar{h}_i (where i is related to the deformation region) can be obtained using the following relations:

$$\bar{h} = \begin{cases} h_0 + \frac{(l-x_{n1})^2}{3R_m} & \text{zone I} \\ h_0 + \frac{(x_{n1}-x_{n2})^2}{3R_m} & \text{zone BII} \\ h_0 + \frac{(x_m-x_{n2})^2}{3R_m} & \text{zone AII} \\ h_0 + \frac{x_{n2}^2}{3R_m} & \text{zone III} \end{cases} \tag{17}$$

The average moment along any deformation zone is given by:

$$\bar{M}_b = \frac{\int_a^b M_b(x) dx}{(b-a)} \tag{18}$$

In any deformation zone, the plate is considered as a beam of uniform thickness \bar{h}_i subjected to bending moment $(\bar{M}_b)_i$. By calculating the radius of curvature due to moment, the resultant curvature is obtained by summation of the developed curvatures at different regions.

$$\frac{1}{\rho_M} = \frac{1}{\rho_I} + \frac{1}{\rho_{AII}} + \frac{1}{\rho_{BII}} + \frac{1}{\rho_{III}} \tag{19}$$

It is assumed that the deformation of plate in the roll gap is similar to a beam subjected to external loading. Considering elasto-plastic material subjected to loading to plastic condition and then unloading, the final curvature after the elastic recovery is.

$$\frac{1}{\rho_{axe}} = \frac{1}{\rho_M} - \frac{1}{\rho_E} \tag{20}$$

where ρ_E is the elastic radius of curvature. In any cross section, the bending moment due to the normal stress is given by:

$$M_b = \int_{-\frac{h}{2}}^{\frac{h}{2}} y \sigma_x dA \tag{21}$$

By definition: $e_x = \frac{y}{\rho_E}$. Substituting for σ_x from Hook's constitutive law into equation (21), the elastic radius of curvature with respect to the internal bending moment, thickness and elastic constants is obtained as follows:

$$\frac{1}{\rho_E} = \frac{12(1-\nu)^2 M_E}{Eh^3} \tag{22}$$

Considering elasto-plastic behavior, the relation between the bending moment and the radius of curvature as given by Johnson et al. (1972) is expressed as follows:

$$12M_b = 3h^2 \sigma_f - 4\sigma_f^3 \frac{\rho_M^2}{E^2} \tag{23}$$

Substitution equation (22) and (23) in equation (20), the outgoing radius of curvature is obtained as follows:

$$\frac{1}{\rho_{axe}} = \frac{2\sigma_f}{E} \frac{1}{\left(3h^2 - \frac{12M_b}{\sigma_f}\right)^{\frac{1}{2}}} - \frac{12(1-\nu^2)M_E}{Eh^3} \tag{24}$$

This curvature is due to the axial strain and is added to the curvature due to the shear strain, so that the final outgoing curvature is given by:

$$\frac{1}{\rho} = \frac{1}{\rho_{axe}} + \frac{1}{\rho_{shr}} \tag{25}$$

Method of calculating the developed curvature $\frac{1}{\rho_{shr}}$, due to shear strain for a rigid-plastic material is the same as the method given in an earlier paper by Salimi et al.(2002). Appendix A presents a method of determining the average yield stress for an elastic-plastic and linear work hardening material.

The curvature index K, defined as the ratio of slab upper surface length divided by slab lower surface length. The relation between ρ and K is given by the following relation:

$$K = \frac{\rho - h_o/2}{\rho + h_o/2} \tag{26}$$

Method of roll force and torque calculation for elasto-plastic and strain hardening material is given in appendix B.

5. Results and discussion

To verify the present analytical model and to study the effect of asymmetrical rolling parameters, the work piece was assumed to have an average yield shear strength of $\bar{k} = 98.2 \text{ MPa}$ and rolled through the rollers of unequal roll radii ($R_2 = 0.9R_1$). A method is presented in appendix A to determine the mean yield stress along the roll gap. Figure (3) illustrates the variation of pressure differences along the contact length for different roll speed ratio. It is indicated that the pressure difference between the rollers increases by increasing the roll speed ratio.

Figure (4) depicts the average pressure along the contact length for different roll speed ratio. By increasing the roll peripheral speed ratios, the length of cross shear zone is also increased. As the mean pressure decreases, the rolling force decreases too.

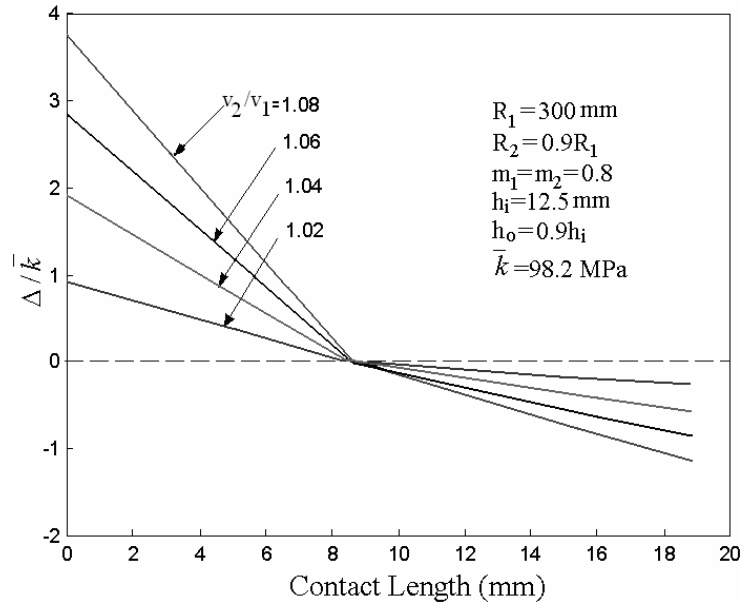


Figure 3. Roll pressure difference distribution along the arc of contact for different speed ratios

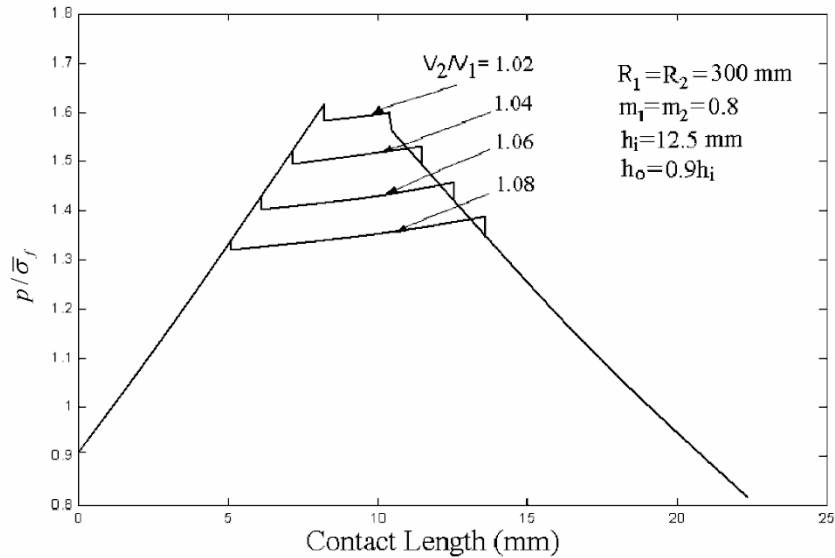


Figure 4. Effect of roller velocity ratio on mean pressure

Figure (5) illustrates the pressure difference along the contact length for different roll diameter ratios. As shown the pressure difference is increased by decreasing the diameter ratio and the pressure difference is more significant for $0 < x < x_m$. By decreasing the radius of one of the rollers, the normal force is distributed along a shorter contact length, thereby the pressure differences is increased.

Figure (6) depicts the variation of pressure difference versus the thickness reduction. By increasing the thickness reduction, the contact length is increased and the pressure difference is decreased. The pressure difference from inlet to middle of the cross shear region is lower than that of the rest of the contact length.

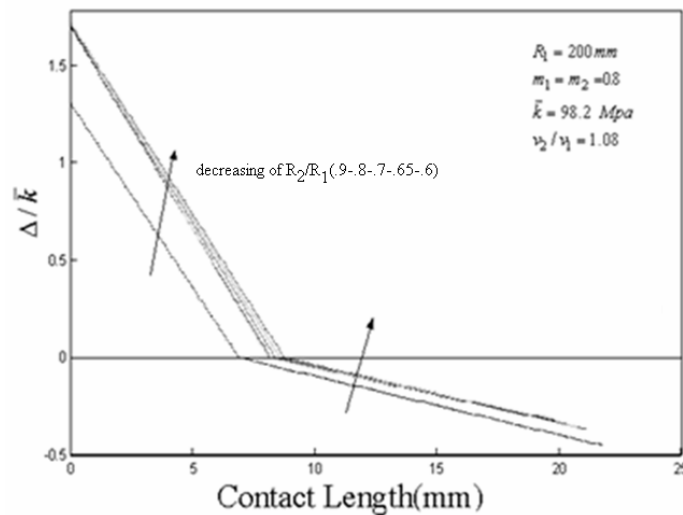


Figure 5. Roll pressure difference distribution for different roll diameter ratios

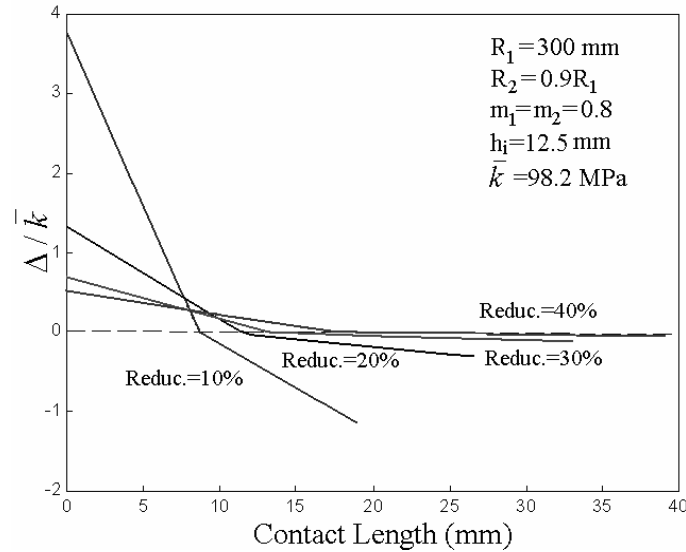


Figure 6. Roll pressure difference distribution for different thickness reduction

Figure (7) illustrates the mean pressure distribution with respect to the thickness reduction. For higher reduction in thickness, the mean pressure is increased as more pressure is needed along the contact length. In addition, it is shown that for lower reduction in thickness, the length of the cross shear zone is longer than that of the higher reductions.

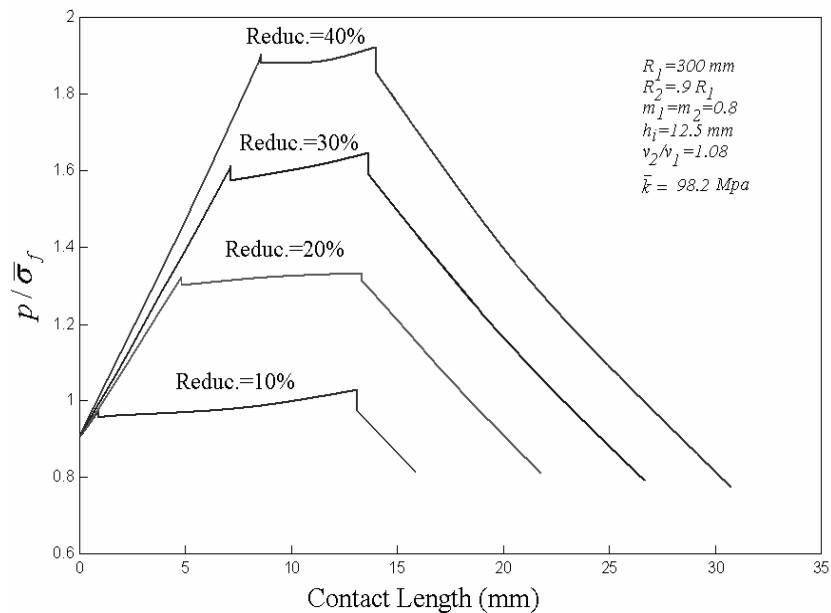


Figure 7. Effect of thickness reduction on distribution of mean pressure

Figure (8) shows the effect of friction factor upon pressure difference distribution. For $m_1/m_2 < 1$, the pressure difference from the middle of cross shear region toward the outlet is positive, but for $x_m < x < 1$ this parameter is negative. Considering the plate as a beam of unequal loading, it is clear that this kind loading, rotates the plate downward. When $m_1/m_2 > 1$, the rotation will be in opposite direction.

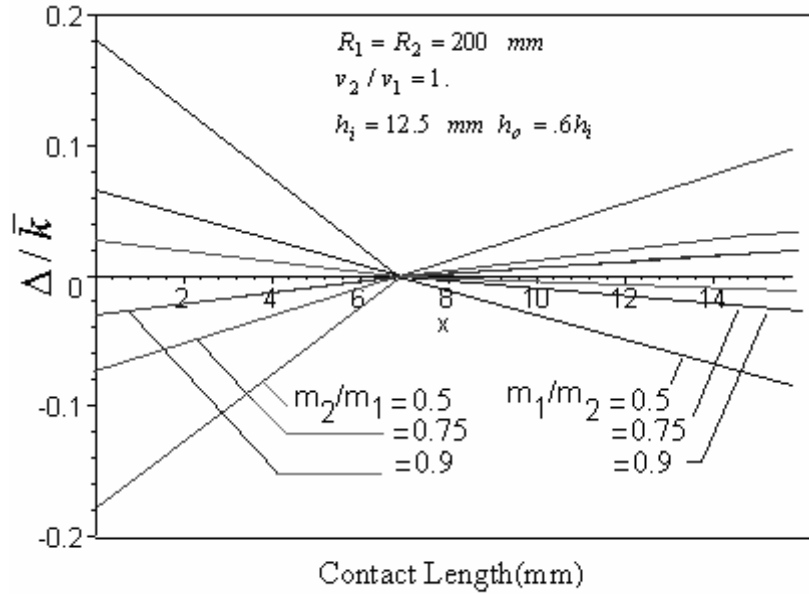


Figure 8. Roll pressure difference distribution for different friction factor ratios

Figure (9) illustrates the effect of forward tension upon curvature index for a constant thickness reduction and different friction factor ratios. As it is shown, the outgoing strip curls towards the roll with higher friction as the smoother roller moves faster than the rough one. This relative motion makes the rotation toward the rougher roll. By applying tension at exit, strip curvature is reduced. Hence, the warping decreases as tension increases.

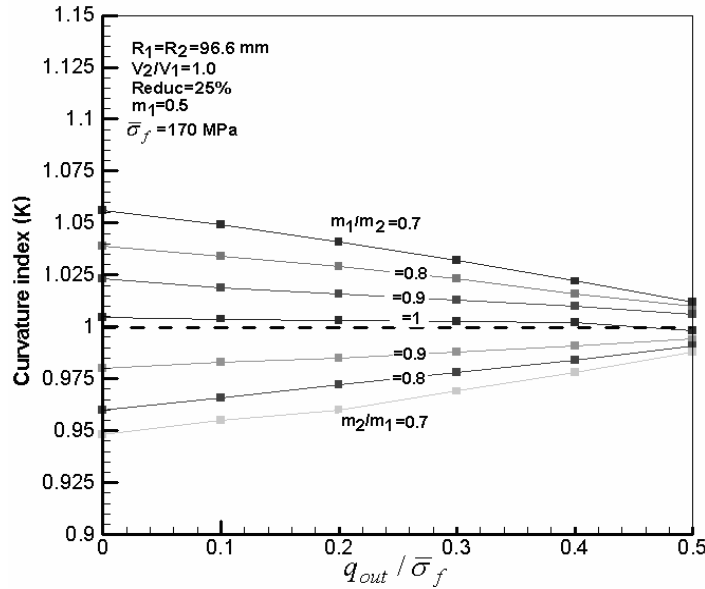


Figure 9. Effect of forward tension on plate curvature

Figure (10) illustrates the effect of bending moment on curvature at entry of the roll gap. Steel strip with an initial thickness of $h_i = 12.5 \text{ mm}$ is rolled with no bending moment at entry (free entry) and a reduction in thickness of 30%. As shown for equal friction factor and equal peripheral velocity, the outgoing strip remain straight (curvature index equal unity). By employing a positive bending moment at entry, the pressure difference is generated between the upper and lower rolls to establish rotational equilibrium. At entry side, the pressure difference is positive and in exit side, this is negative. Under this situation, a positive coupling is created due to the pressure difference and bends the plate toward the upper roll ($K > 1$). Applying a negative bending moment to the plate bend the plate downward ($K < 1$).

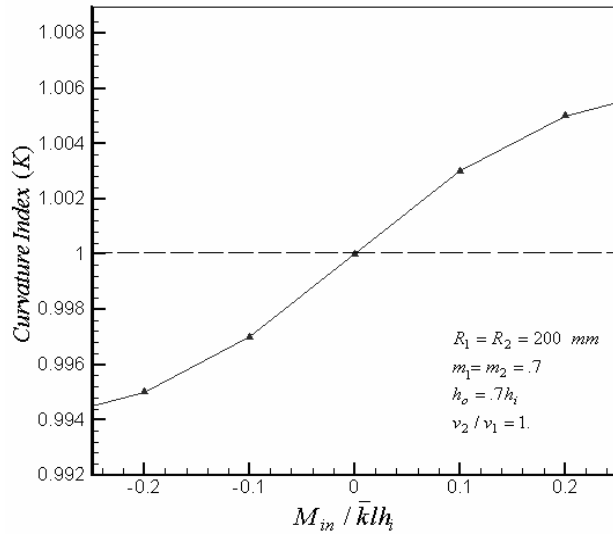


Figure 10. Effect of bending moment at entry to curvature index for identical friction factors

Figure 11 show the same effect where the plate rolled under the same condition except that the friction factor of the upper roll is different. With no bending moment at entry, warping is toward the upper roll. Application of negative bending moment reduces the amount of curvature while positive moment increases the curvature.

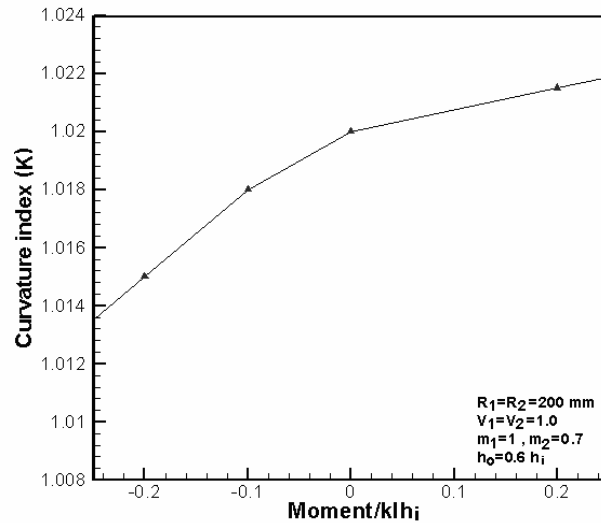


Figure 11. Curvature indexes versus bending moment at entry for different friction factors

The effect of inlet bending moment on pressure difference is examined in Figure 12. Asymmetry was created due to the difference in friction factors, with no bending moment at the entry, pressure difference in $x_m < x < l$, is positive ($p_1 > p_2$) and for $0 < x < x_m$ pressure difference is negative ($p_1 < p_2$). By applying positive bending moment, the pressure difference for maintaining the rotational equilibrium in both area is increased and it is positive for $x_m < x < l$ and negative for $0 < x < x_m$. Application of negative moment at entry has a negative effect on this parameter.

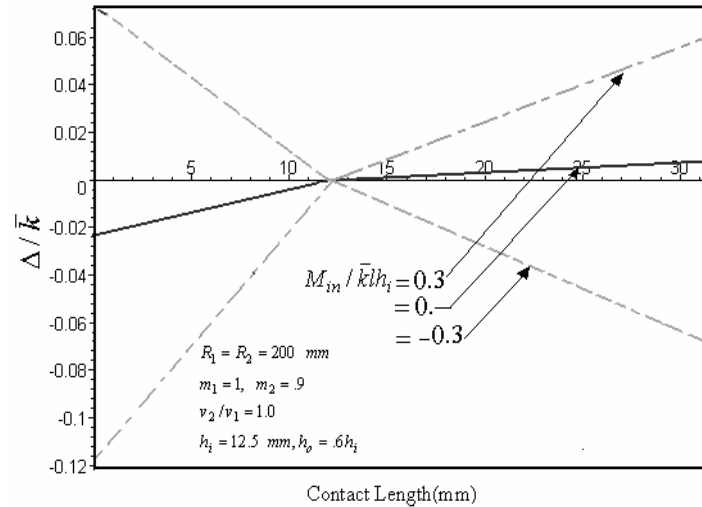


Figure 12. Roll pressure difference distribution for different bending moment at entry of roll gap

In Figure (13) the effect of front tension upon the variation of average pressure is given. By increasing the front tension, the average pressure decreases. In addition, the neutral points move toward the entry of roll gap. By increasing the strip tension the average pressure is reduced thus, the separating roll force is decreased.

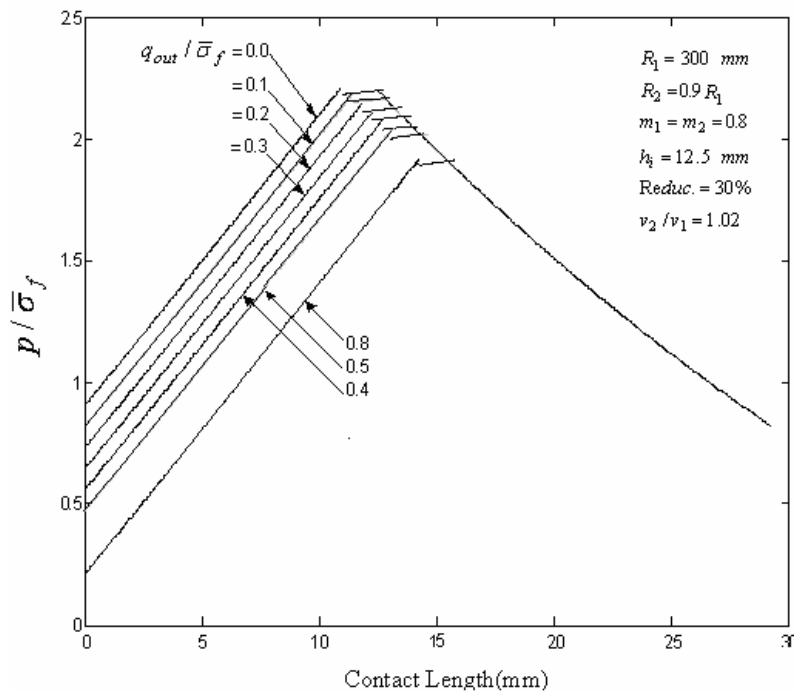


Figure 13. Effect of forward tension on mean pressure

In Figure 14, the variation of average pressure is plotted versus the variation of back tension. By increasing the back tension, the average pressure is decreased. As a result, the roll separating force decreases. The location of neutral points moves toward the exit of roll gap.

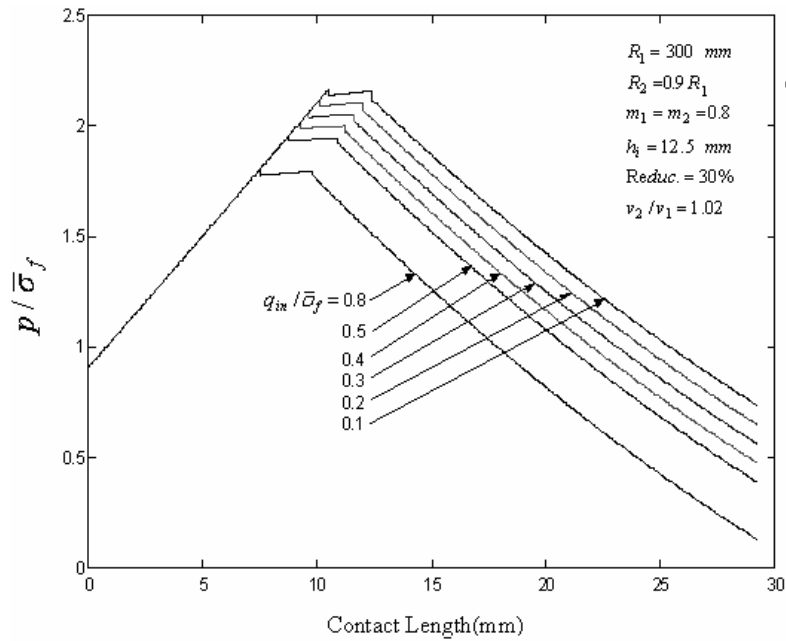


Figure 14. Effect of backward tension on mean pressure

It is concluded from Figures 13 and 14 that application of forward and backward tension decreases the roll separating force. As it is shown in both Figures, the length of cross shear zone is not affected by backward or frontward tension. Comparison of results for the current model, Hwang et al. (1996) and their experimental values are shown in Figures 15 and 16. Since in present model, the effect of shear stress across the thickness is considered, the predicted values of the model for the rolling force and torque are closer to the experimental values.

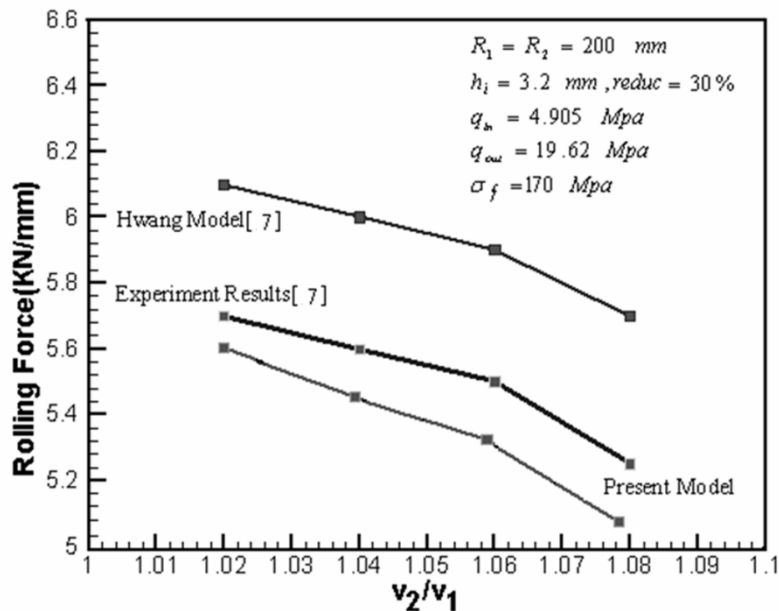


Figure 15. Comparison between evaluated rolling force in the present model with Hwang model and experimental results

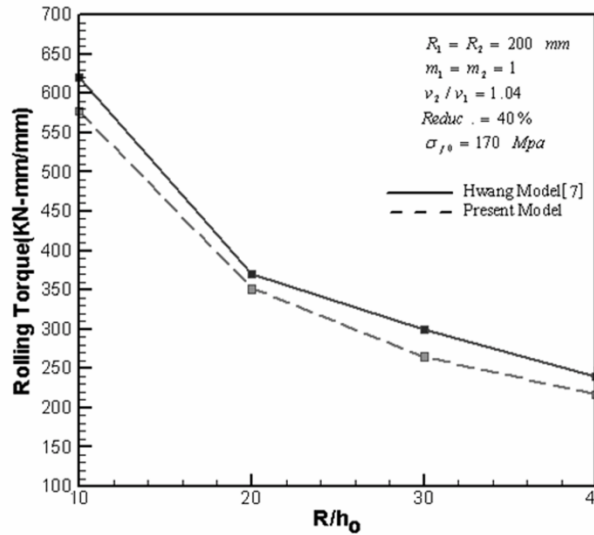


Figure 16. Comparison between evaluated rolling torque in the present model with Hwang model and experimental results

6. Conclusion

This paper has presented an analysis using the modified slab method to study a wide range of asymmetrical rolling. Following are some of the concluding remarks:

1. Increasing the roll diameter ratio increases the pressure differences, but the average pressure to the rolls will decrease.
2. By increasing the reduction in thickness, the pressure difference will decrease and the average pressure will increase.
3. To decrease warping, bending moment may be applied in a suitable direction. If all conditions at the top and bottom rollers are the same but only $v_2 > v_1$, application of positive bending moment decreases the pressure difference and advances the rolling process toward the symmetrical condition. If only the friction factors are different; $m_1 > m_2$, the pressure difference will increase.
4. Applying front or back tension results in decreasing of average pressure distribution and moves the position of the neutral points towards to entry or exit. In addition, by applying the front tension the outgoing sheet warping will decrease.
5. Applying bending moment at entry of the roll gap in a symmetrical rolling process causes pressure difference on the rolls and warping in outgoing sheet, as it happens in an asymmetrical rolling process.
6. The length of cross shear zone depends on peripheral speed ratio, thickness reduction, shape factor (length per average height) and other input variables.

Appendix A

Determination of average yield stress for elasto-plastic and linear strain hardening material

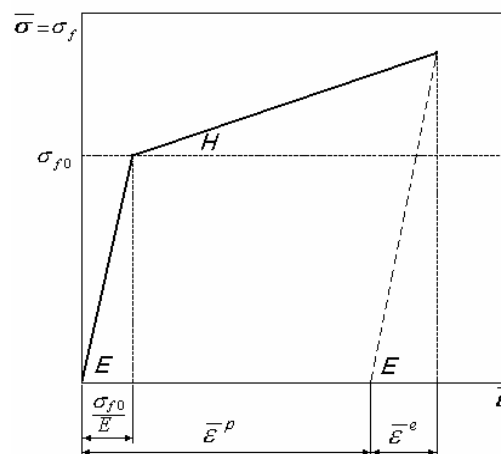


Figure (A-1) stress-strain curve of an elasto-plastic material with linear strain hardening

By referring to Figure (A), the yield stress is function of the effective strain, while for an elasto – plastic material; total strain $\bar{\epsilon}$ is the summation of elastic and plastic strains, $\bar{\epsilon}^e$ and $\bar{\epsilon}^p$:

$$\bar{\epsilon} = \bar{\epsilon}^e + \bar{\epsilon}^p \tag{A-1}$$

$$\sigma_f = \sigma_{f0} + H\left(\bar{\epsilon} - \frac{\sigma_{f0}}{E}\right) \tag{A-2}$$

The effective strain is the summation of elastic and plastic effective strains. Assuming plane strain condition and volume constancy we have:

$$d\bar{\epsilon} = d\bar{\epsilon}^e + \frac{2}{\sqrt{3}}d\bar{\epsilon}_x^p \tag{A-3}$$

By dividing of the plate to upper and lower portion based on different characteristics of distribution of shear strain along the thickness, principal strain in any portion is obtained as follows:

$$d\bar{\epsilon}_{1,2} = \mp (d\bar{\epsilon}_y)_h \sqrt{1 + \frac{\eta^2}{4}}, \quad \eta = \frac{mc}{(1-m^2c^2)^{\frac{1}{2}}} \tag{A-4}$$

In above equation, c may be replaced by c1 or c2 based on Salimi et al. (2002). Effective plastic strain can be obtained as a function of thickness in any distance from the exit, as follows:

$$\bar{\epsilon}^p(x) = \frac{2}{\sqrt{3}}\zeta \ln \frac{h_i}{h(x)} \tag{A-5}$$

$$\zeta = \frac{1}{2} \left(\frac{1 - \frac{3}{4}m^2c^2}{1 - m^2c^2} \right)^{\frac{1}{2}} \tag{A-6}$$

Hence, the yield stress in upper portion of sheet can be determined as follows:

$$\sigma_{f1}(x) = \sigma_{f0} + \frac{H}{1 - \frac{H}{E}\sqrt{3}} \frac{2}{\sqrt{3}} \zeta \ln \frac{h_i}{h(x)} \tag{A-7}$$

Practically, ζ is not much different at the top and bottom portion, thus the average yield stress in upper and lower portion of sheet is approximately the same.

$$\bar{\sigma}_f = \frac{\int_0^l \sigma_f dx}{l} \tag{A-8}$$

The average of yield stress along the contact length is determined as follows:

$$\bar{\sigma}_f = \sigma_{f0} + (2\zeta) \left(\frac{H}{\sqrt{3}} \right) \left(\frac{1}{1 - \frac{H}{E}} \right) \left(\ln \frac{h_i}{h_o} + 2 - 2 \frac{1}{\omega} m^{-1} \omega \right), \quad \omega = \frac{l}{\sqrt{R_m h_0}} \tag{A-9}$$

Appendix B

Determination of roll force and torque for elasto-plastic and strain hardening material

The rolling load can be obtained by integrating from the roll pressure $p = I_1 + I_2x - q$ where q is given by equation (13-2) and the coefficients J_{1q} , J_{2q} and J_{3q} are given in equation (14). The rolling torque exerted to the upper and lower rolls can be calculated by integrating from the torque applied by frictional stress along the arc of contact around each roll axis:

$$T = \int_0^l mk(x)Rdx = \int_0^l mR \left\{ k_0 + \frac{\frac{2}{3}H}{1 - \frac{H}{E}} \zeta \ln \frac{h_i}{h(x)} \right\} dx \quad (\text{B-1})$$

Total rolling torque is the summation of upper and lower torque of rollers:

$$T = T_1 + T_2 \quad (\text{B-2})$$

$$T_1 = m_1 R_1 (k_0 + 2\xi_1)(l - 2x_{n1}) - 2\xi_1 x_{n1} \ln \frac{h_i}{h_1} - \frac{2\xi_1 l}{\omega} \left\{ \tan^{-1} \omega - 2 \tan^{-1} \frac{\omega x_{n1}}{l} \right\} \quad (\text{B-3})$$

$$T_2 = m_2 R_2 (k_0 + 2\xi_2)(l - 2x_{n2}) - 2\xi_2 x_{n2} \ln \frac{h_i}{h_2} - \frac{2\xi_2 l}{\omega} \left\{ \tan^{-1} \omega - 2 \tan^{-1} \frac{\omega x_{n2}}{l} \right\} \quad (\text{B-4})$$

In this equation ξ is defined as follows:

$$\xi = \frac{\frac{2}{3}H\zeta}{1 - \frac{H}{E}} \quad (\text{B-5})$$

References

- Chekmarev, A.P. and Nefedov, A.A., 1956. *Obrabotka Metallov Davleniem*, British Library Translation, R.T.S. 8939.
- Collins, I.F. and Dewhurst, P., 1975. A slip-line field analysis of asymmetrical hot rolling, *Int. J. Mech. Sci.*, Vol.17, pp. 643.
- Dyja, H., Korczak, P., Pilarczyk, J.W., and Grzybowski, J., 1994. Theoretical and experimental analysis of plates asymmetrical rolling, *J. Materials Processing Technology*, Vol. 45, pp. 167- 172.
- Farhatnia, F. and Salimi, M., 2005. Clad Sheet Rolling Analysis by Modified Slab Method, *Proceedings of the Int. Conf ESAFORM 8, Cluj-Napoca*, pp.1125-1130.
- Farhatnia, F. and Salimi, M., 2006. An analytical approach to clad sheet rolling by modified slab method, *Proceeding of 13th Asia Steel Conference*, Fukuoka, Japan.
- Farhatnia, F. and Salimi, M., Movahhedy, M.R., 2006. Elasto-plastic finite element simulation of asymmetrical plate rolling using an ALE approach, *Int. J. Materials Processing Technology*, Vol.77, No. 1-3, pp. 525-529.
- Gudur P.P., Salunkhe M.A., and Dixit, U.S., 2008. A theoretical study on the application of symmetric rolling for the estimation of friction, *Int. J. Mechanical Science*, Vol. 50, pp. 315-327.
- Hwang Y.W. and Chen T.H, 1996. Analysis of asymmetrical rolling by stream function method, *JSME* Vol.39, P. 598.
- Hwang, Y.W. and Tzou, G.Y., 1997. Analytical and experimental study on asymmetrical sheet rolling, *Int. J. Mechanical Science*, Vol. 39, pp. 289-303.
- Kiuchi, M.M. and Hsiang, S., 1986. Analytical model of asymmetrical rolling process of sheets, *Proc. 14th NAMRC, Society of Manufacturing Engrs, Minneapolis*, pp. 384.
- Knight C. W., Hardy S. J. and Lees A.W., 2003. Investigations into the Influence of Asymmetric Factors and Rolling Parameters on Strip Curvature During Hot Rolling, *J. of Materials Processing Technology*, Vol.134, pp. 180-189.
- Knight, C.W., Hardy, S.J., Lees, A.W. and K.J. Brown 2005. Influence of roll speed mismatch on strip curvature during the roughing stages of a hot rolling mill, *Int. J. Materials Processing Technology*, Vol.168, pp. 184-188.
- Lu, L.S., Harrer, O.K., Schwenzfeier, W. and Fischer, F.D., 2000. Analysis of the bending of the rolling material in asymmetrical sheet rolling, *Int. J. Mechanical Science*, Vol. 42, pp. 49-61.
- Mousavi, S.S.A., Ebrahimi, S. M. and Madoliat, R., 2007. Three dimensional numerical analyses of asymmetric rolling, *Int. J. Material Processing and Technology*, 187-188 pp. 725-729.
- Pan, D., and Sansome, D.H., 1982. An experimental study of the effect of roll-speed mismatch on the rolling load during the cold rolling of thin strip, *J. Mech. Tech.*, Vol.6, pp 361.

- Richelsen, A.B., 1997. Elastic-plastic analysis of the stress and strain distributions in asymmetric rolling, *Int. J. Mechanical Science*, Vol. 39, P. 1199.
- Salimi, M., and Sassani, F., 2002. Modified slab analysis of asymmetrical plate rolling, *Int. J. Mech. Sci.*, 44, pp. 1999-2023.
- Shivpuri, R., Chou, P.C. and Lau, C.W., 1988. Finite element investigation of curling in nonsymmetrical rolling of sheet *Int. J. Mech. Sci.*, 30, P. 625.
- Johnson, W. and Mellor P.B., 1972. *Engineering Plasticity*, John Willey & Sons.

Biographical notes

Dr. F. Farhatnia has obtained her PhD from Isfahan University of Technology, Isfahan, Iran from the Department of Mechanical Engineering in 2005. She is presently working as an Assistant Professor in the Islamic Azad University of Khomeini-Shahr. Her research interest includes: stability analysis of FGM structures, elasticity, rolling process in metal forming and stress analysis.

Prof. M. Salimi has obtained his PhD from University of Manchester Institute of science and Technology, in UK. He is a professor in Mechanical Engineering. His area of expertise is Mechanics of Deformable Bodies, Fracture and Damage, Plasticity and Metal Forming.

Received October 2010

Accepted June 2011

Final acceptance in revised form June 2011